Impact of Ca/(Si+Al) Ratio of Calcium Aluminosilicate Hydrate (C-A-S-H) Gel on Chloride Adsorption for Evaluating Durability of Reinforced Concrete

Kobayashi[1] H, *Yogarajah[2] E and Nawa[2] T

[1]Graduate School of Engineering, Hokkaido University, Japan
[2]Faculty of Engineering, Hokkaido University, Japan
*Corresponding author – elakneswaran@eng.hokudai.ac.jp

Abstract

Cement-based materials have been using in various application of reinforced concrete structural components as well as in nuclear waste repositories. The ingress of detrimental ions and consequent chemical reactions pose severe threat to the durability of cementitious materials. The chloride-induced corrosion in concrete structures is one of serious durability problems. In the penetration of chloride into concrete, it is necessary to consider both binding and diffusion of chloride. The adsorption of chloride on the surface calcium silicate hydrate (C-S-H) gel, main hydration product of cement, controls the binding of chloride in cement-based materials. It has been reported that a partial substitution of Portland cement by ground granulated blast furnace slag(GGBFS) increase the chloride adsorption and form C-A-S-H gel. The physicochemical and surface electrical properties of C-A-S-H gel are significantly different from the properties of C-S-H gel. Therefore, in this study, chloride adsorption behavior on C-A-S-H gel is analyzed by experimental techniques. The C-A-S-H gel with different Ca/ (Si+Al) ratios was synthesized and their structure and active surface site were analyzed by ^{29}Si MAS-NMR and ^{27}Al MAS-NMR. And zeta potential of C-A-S-H gel in various suspensions were measured and the chloride adsorption experiment was conducted on C-A-S-H gel.

Keywords: C-A-S-H gel, Ca/(Si+Al) ratio, ^{29}Si MAS-NMR, ^{27}Al MAS-NMR, Zeta potential, Chloride adsorption

1. Introduction

The chloride-induced corrosion of reinforcement in concrete structures caused by chloride ions in sea water or others is a problem as a cause of early deterioration of concrete, and it is caused by chloride ions penetrating and diffusing into the reinforced concrete. Therefore, in evaluating the influence of chloride ions, it is important to accurately obtain the diffusion and immobilization behavior of chloride ions in concrete. In general, in the immobilization of chloride ion, physical adsorption to C-S-H, main hydration product of cement, is predominant. Physical adsorption to C-S-H is believed to occur at the SiOH site on the C-S-H surface. According to Pointeau et al.[1], there are two types of SiOH site : a silanol site (Q^1) present at the pairing position of the SiO_4 tetrahedral chain and a silanediol site (Q^2_b) present at the bridging position.

Figure 1 shows the structural concept of SiO_4 tetrahedral chains in C-S-H [2]. Q^1 and Q^2 in the figure indicate spectra representing the structure of the SiO_4 tetrahedron of C-S-H in ^{29}Si MAS-NMR, Q^1 is at the chain-end position, and Q^2 is in the chain of the SiO_4 tetrahedra. Q^2 is classified into Q^2_b (coordinated to H^+) at the bridging position and Q^2_p (coordinated to the Ca-O sheet). It is reported that these SiO_4 tetrahedra can be quantified to each bonding state (Q^1, Q^2_b,...) by ^{29}Si MAS-NMR spectrum analysis [3].

The dissociation degree of H^+ differs depending on the pH of the SiOH site, whereby the charge on the C-S-H surface changes. In addition, the Q^1 site is bound to one Si^{4+} via an oxygen atom O, whereas the Q^2_b site is bound to two Si^{4+} sites via two oxygen atoms O, it is predicted that the amount of charge will be different. These surface sites each have dissociation constants of different deprotonation, and when H^+ is eliminated, it becomes a negative charge and becomes a surface site. Then, Ca^{2+} adsorbs to the deprotonated site, thereby positively charges and becomes a chloride ion adsorption site.

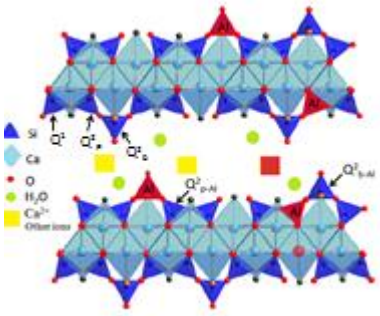

Figure. 1 - Existence form of Si tetrahedron (14Å tobermorite) [3].

Many predictive modeling of the amount of physical adsorption of chloride ions to C-S-H by determining the equilibrium constant in these reactions by using the surface complex model has not been completed accurately in any of the models . One reason is that the characterization of the SiOH site is insufficient. According to Churakov et al.[4], the SiOH sites belonging to the Q^1 and Q^2_b sites can be regarded as having two kinds of bonding angles, respectively, and in the simulation performed by Churakov et al., four types of ≡SipO^{1}H, ≡SipO^{2}H, ≡SibO^{1}H, ≡SibO^{2}H of SiOH sites (Figure 2). However, distinction between these four kinds of SiOH sites is not sufficiently considered.

On the other hand, it has been reported that the structure of C-S-H changes due to Ca/Si ratio, Al addition ratio, synthesis temperature, and the like. For example, according to Richardson[3], an increase in the Ca/Si ratio results in the loss of the Q^2_b. It has also been reported that Q^2_b is substituted from Si^{4+} to Al^{3+} in the system and C-S-H becomes C-A-S-H where Al is present such as GGBFS [5].

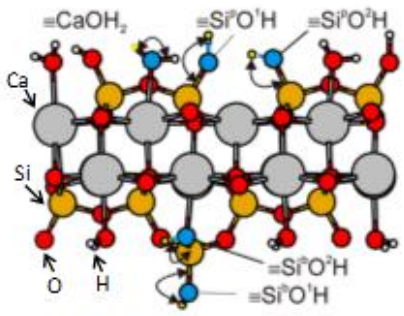

Figure. 2 - Schematic view on the C-S-H surface [4].

It is thought that such a structural change affects the surface charge of C-A-S-H and the physical adsorption amount changes. According to Faucon et al.[6], $Si^{4+} \rightarrow Al^{3+}$ substitution occurs not only at the bridging position of the SiO_4 tetrahedron but also at the pairing position and between the layers of the Ca-O sheet and the layer.

Therefore, in this study, C-A-S-H with different Ca/(Si+Al) ratio was synthesized and structure study of C-A-S-H was conducted by using ^{29}Si MAS-NMR and ^{27}Al MAS-NMR. Hereinafter, as shown in Figure 1, when Si at the bridging position is replaced with Al, it is written as $Q^2_{b\ Si\rightarrow Al}$, and the Si adjacent to it is written as $Q^2_{p\ -Al}$. Also, when Si in the pairing position is replaced, it is written as $Q^2_{p\ Si\rightarrow Al}$, and the Si adjacent to it is written as $Q^2_{b\ -Al}$. Further, when Si at Q^3 position is replaced, it is written as $Q^3_{Si\rightarrow Al}$, and the Si adjacent to it is written as Q^3_{-Al}.

2. Methodology

2.1 Materials

Samples used were adjusted so that Ca/(Si+Al)=0.8, 1.0, 1.4, respectively, substituting SiO_2 with $CaAl_2O_4$ by 2, 4, 8, 16%. Subsequently, a sample with Ca/(Si+Al) = x and $CaAl_2O_4$ substitution rate of y% is described as CASH-x-Ay. $Ca(OH)_2$ (Kanto Chemical Co., Ltd., special grade reagent), SiO_2 (Nippon Aerosil Co., Ltd., AEROSIL 200, purity: 99.9% or more), $CaCO_3$ (Kanto Chemical Co.), Al_2O_3 (Kanto Chemical Co., special grade reagent) was used. Calcined CaO, SiO_2 and calcined $CaAl_2O_4$ were mixed with distilled water according to the stoichiometric ratio so as to have a water powder ratio of 45 (ml/g) and synthesized. CaO and $CaAl_2O_4$ was calcined by Myers's method[2]. After that, N_2 gas was sealed, curing was carried out for 5 weeks in a thermostatic chamber at 80 ℃, and the container was shaken twice a week (once every 1 hour for the first 3 hours). Recovery was performed by suction filtration, washed once with distilled water and ethanol mixed 1: 1, and lyophilized for 1 day or more. Table 1 shows the composition of each sample measured by XRF. A diffraction diagram of tobermorite by XRD measurement was obtained in the same manner as in the past study, and it was confirmed that tobermorite type C-A-S-H was synthesized[2].

2.2 Methods

2.2.1 ^{29}Si MAS-NMR and ^{27}Al MAS-NMR spectral analysis

Chemical shifts of C-A-S-H with different Ca/(Si+Al) ratios were measured using $[(Si(CH_3)_3]_8Si_8O_{20}$ and $AlCl_3 \cdot 6H_2O$ as reference materials for ^{29}Si and ^{27}Al spectra, respectively. For the measurement of the ^{29}Si spectrum, MSL-400 (Bruker) was used with a 90° pulse width of 5 μs, a flip angle of π/6, a waiting time of 20 s, and a 7 mm MAS probe was used to measure at 4 kHz. For the measurement of the ^{27}Al spectrum, ECA-700 (JEOL) was used, measuring 90° pulse width 2.14 μs, flip angle π/6, waiting time 30 s, using a 3.2 mm MAS probe at a rotation frequency of 18 kHz. The measurement conditions of both spectra were set so that the slowest peak of relaxation was sufficiently saturated. The measured spectrum was decomposed using the Lorenz function, and the abundance ratios of Q^1, Q^2_p, Q^2_b, etc. were calculated from the obtained peak area. In addition, WinNuts was used for analysis of ^{29}Si spectrum, and Delta was used for analysis of ^{27}Al spectrum.

Table 1 - Experimental parameters and conditions used

Sample	CaO (mol)	SiO_2 (mol)	$CaAl_2O_4$ (mol)	Initial Ca/(Si+Al)	Ca/(Si+Al) by XRF	Initial Al/Si	Al/Si by XRF
CASH-0.8-A2	0.77	0.91	0.02	0.8	0.80	0.042	0.053
CASH-0.8-A4	0.79	0.88	0.03	0.8	0.85	0.087	0.066
CASH-0.8-A8	0.79	0.85	0.05	0.8	0.84	0.190	0.109
CASH-0.8-A16	0.84	0.76	0.07	0.8	0.92	0.471	0.186
CASH-1.0-A2	0.95	0.68	0.03	1.0	1.28	0.042	0.089
CASH-1.0-A4	0.90	0.75	0.05	1.0	1.07	0.087	0.123
CASH-1.0-A8	0.94	0.67	0.07	1.0	1.16	0.190	0.210
CASH-1.0-A16	0.90	0.62	0.09	1.0	1.12	0.471	0.293
CASH-1.4-A2	0.98	0.70	0.03	1.4	1.28	0.042	0.082
CASH-1.4-A4	0.97	0.69	0.04	1.4	1.26	0.087	0.119
CASH-1.4-A8	0.98	0.65	0.06	1.4	1.29	0.190	0.184
CASH-1.4-A16	1.05	0.55	0.08	1.4	1.47	0.471	0.308

Also, with reference to the method of Pardal et al.[9], associate the amount of Al in the SiO_4 tetrahedral chain ($Q^2_{p\ Si\rightarrow Al}$, $Q^2_{b\ Si\rightarrow Al}$, etc.) such as the amount of substitution of Si→Al to Q^2_b, Q^2_p, etc. obtained from the spectrum of ^{27}Al and the amount of each Si bonding state in the SiO_4 tetrahedral chain (Q^1, Q^2_p, etc.) obtained from the spectrum of ^{29}Si quantitative and structural studies were carried out. At this time, the composition ratio of each element in C-A-S-H was in accordance with the result of XRF measurement.

2.2.2 Zeta potential measurement

In this study, in order to measure the influence of the change in surface potential of Ca/(Si+Al) ratio of SiOH site in SiO_4 tetrahedral chain, the change in ζ potential of each sample in a solution with pH changed was investigated. A fine powder sample was immersed in a NaOH aqueous solution, a Ca $(OH)_2$ aqueous solution and an NaCl aqueous solution whose ionic strength was uniformly adjusted with $NaNO_3$ so that a suspension having a solid-liquid ratio of 0.1 g/L was obtained. After immersing the sample for 24 hours, the suspension was dispersed by an ultrasonic shaker before measurement. The concentrations of NaOH aqueous solution and Ca $(OH)_2$ aqueous solution were 0.1, 1, 5 mM, and the concentration of NaCl aqueous solution was 1, 5, 10 mM. In addition, Ca $(OH)_2$ was added to the NaCl aqueous solution at 5 mM to prevent dissolution (Ca leaching) of the sample. Each solution measured 5 times, by using a laser Doppler method. The measurement temperature was 25 ℃, and one cell measured 3 times. The pH of the solution was measured 3 times, and the average was taken as the pH of each solution. Each measurement result is sectioned with a zone of ζ potential 4 mV, and the area of ζ potential intensity observed in that interval is calculated. This was carried out for a total of 15 measurement results for each sample and each concentration, and the average value was obtained to obtain the frequency of the area in each ζ potential section,

and the frequency in that section was plotted at the midpoint of each ζ potential section . Thereafter, fitting by the normal distribution was performed with respect to the obtained frequency, and the peak of the normal distribution was taken as the ζ potential at each pH.

3. Results and Discussion

3.1 ^{29}Si MAS-NMR and ^{27}Al MAS-NMR spectral analysis

An example of waveform separation of ^{27}Al MAS-NMR spectrum is shown in Figure 3, ^{27}Al MAS-NMR spectrum is shown in Figure 4, and analysis results are shown in Table 2. The ^{29}Si MAS-NMR spectrum is shown in Figure 5, and the analysis result is shown in Table 3 (A2 and A16 series are shown). As a result of measurement considering saturation of the slowest relaxation peak in this study, four types of IV coordination peaks were confirmed in ^{27}Al MAS-NMR (see Figure 3). Among them, a broad peak at 60 to 70 ppm and a sharp peak at around 72 ppm (IVa and IVb2 in Figure 3) are reported by Pardal et al[8]. A broad peak (IVa) of 60 to 70 ppm is believed to be a state where Al is incorporated in the Q^2_b position[8]. On the other hand, a sharp peak (IVb2) of 72 ppm is thought to be a state in which Al is incorporated in the Q^2_p position[8]. But, since reports on the other two peaks (IVb1, IVc in Figure 3) were not found, based on the measurement results of ^{29}Si MAS-NMR and ^{27}Al MAS-NMR spectra and the influence on the structure due to the change in Ca/(Si+Al) ratio, it is estimated what kind of bonding state each peak corresponds.

First, in Ca/(Si+Al) = 0.8, since the SiO_4 tetrahedral chain length was long by ^{29}Si MAS-NMR and the peak

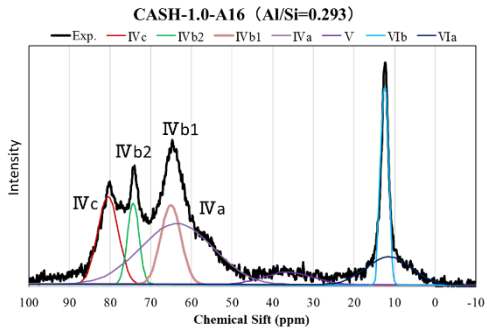

Figure 3 - Example of waveform separation of ^{27}Al MAS-NMR spectra

Table 2 - Results of ^{27}Al MAS-NMR spectra analysis (A2 and A16 series)

	IVc	IVb	IVa	V	VI
CASH-0.8-A2	31.48	0.00	36.89	9.84	21.80
CASH-0.8-A16	12.73	0.00	46.07	3.88	37.32
CASH-1.0-A2	3.52	26.06	51.44	4.96	14.02
CASH-1.0-A16	14.79	21.16	36.64	4.50	22.91
CASH-1.4-A2	7.79	14.02	43.61	9.35	25.23
CASH-1.4-A16	0.00	4.01	47.56	0.00	48.43

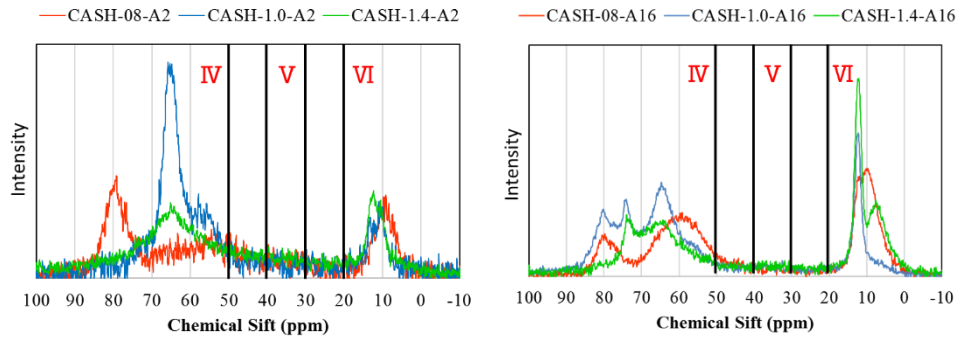

Figure 4 - ^{27}Al MAS-NMR spectra (left : A2 series, right : A16 series)

around 74 ppm was not observed by ^{27}Al MAS-NMR, it is inferred that the peak of IVb1 is considered to be a part in which Al is difficult to be taken in when the SiO_4 tetrahedral chain length is long. Here, it is known that incorporation of Al into both Q^2_p and Q^2_b adjacent to Q^2_p or Q^2_b is difficult compared with incorporation of Al into only Q^2_p or Q^2_b. Next, with Ca/(Si+Al)=1.4, Q^3 was not confirmed by ^{29}Si MAS-NMR and the peak around 80 ppm was not observed by ^{27}Al MAS-NMR, the peak of IVc was Q^3 it is understood that it has a correlation with the position. That is, it can be inferred that Al was incorporated in the Q^3 position. In the analysis result of Table 2, the combination of IVb1 and IVb2 is taken as IVb, and VIa and VIb together are taken as VI. In the analysis of ^{29}Si MAS-NMR spectrum, Al(IVc) taken in Q^3 position and Si adjacent to Q^3 position are $Q^3_{\text{-Al}}$, Al(IVb1, IVb2) taken in Q^2_p position and Si adjacent to Q^2_b position are $Q^2_{\text{b-Al}}$, Al(IVa) taken in the Q^2_b position and Si adjacent to Q^2_p position as $Q^2_{\text{p-Al}}$, analysis was performed in association with ^{27}Al MAS-NMR. As a result, as the Ca/(Si+Al) ratio increases, the crosslinked part decreases and the SiO_4 tetrahedral chain becomes shorter, the crosslinked part increases with the increase of the Al $CaAl_2O_4$ addition ratio, and the SiO_4 tetrahedral chain it was confirmed that it became longer. Note that the analysis results in Table 3 show the ratio when Si and Al in the tetrahedral SiO_4 tetrahedral chain are taken as 100%.

3.2 Zeta potential measurement

Fig 6 shows the results of plotting the normal distribution to the frequency distribution of each area and plotting the ζ potential of the obtained peak with respect to the pH of each solution. From the result of ζ potential when immersed in NaOH, two different peaks of ζ potential were observed in some samples, and it was confirmed that there were sites having different surface charges. In the sample two peaks are confirmed, one peak

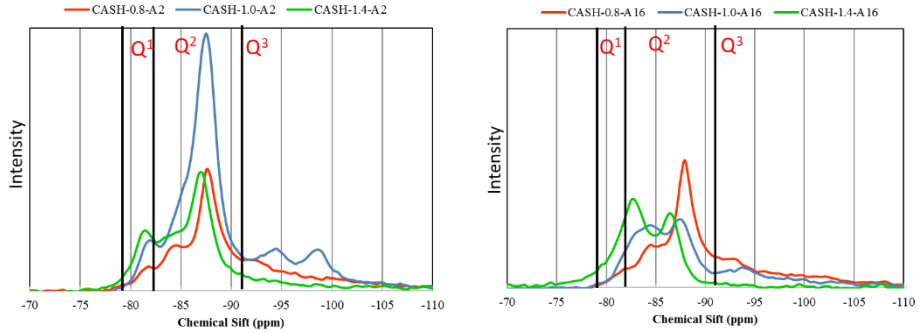

Figure 5 - ^{29}Si MAS-NMR spectra (left：A2 series, right：A16 series)

Table 3 Results of ^{29}Si MAS-NMR spectra analysis（A2 and A16 series）

	Q^1	Q^2_b	$Q^2_{\text{b-Al}}$	$Q^2_{\text{b Si→Al}}$	Q^2_p	$Q^2_{\text{p-Al}}$	$Q^2_{\text{p Si→Al}}$	Q^3	$Q^3_{\text{-Al}}$	$Q^3_{\text{Si→Al}}$
CASH-0.8-A2	11.47	25.18	0.00	0.96	52.28	1.08	0.00	7.89	0.72	0.41
CASH-0.8-A16	10.28	21.71	0.00	4.09	53.21	1.99	0.00	7.82	0.33	0.56
CASH-1.0-A2	10.92	24.32	0.35	2.77	47.07	3.80	0.56	6.67	3.47	0.08
CASH-1.0-A16	17.62	33.46	0.44	6.31	28.10	8.51	1.41	2.89	0.26	0.99
CASH-1.4-A2	31.38	24.83	0.64	2.04	38.44	2.39	0.28	0.00	0.00	0.00
CASH-1.4-A16	30.44	20.66	0.53	7.08	33.73	7.27	0.29	0.00	0.00	0.00

intensity is considerably low, its frequency is less than 10%, and this low peak is written as "CASH-0.8-A2 low" (ignoring less than 1%). It is considered that the surface potential of C-A-S-H is not influenced by the bridging amount or Al replacement amount because almost equal ζ potential was obtained regardless of the Ca/(Si+Al) ratio in the peak with high intensity. Furthermore, since the change in surface charge accompanying pH change is also small, it was assumed that dissociation of the surface site generating the surface potential hardly occurred. Churakov et al.[4] showed that dissociation of H^+ from SiOH sites tends to occur at Q^2_b rather than Q^1, and when dissociating into two kinds of surface sites, site Q^2_b, which is susceptible to dissociation, suggested that deprotonation was occurring at pH=9 and above. From this, it is assumed that the surface potential observed at pH = 9 and above in this study was caused by dissociation of H^+ from SiOH site at Q^1. If the surface potential is generated by dissociation of H^+ from the SiOH(AlOH) site at Q^2_b, the influence of the bridging amount accompanying the change of the Ca/(Si+Al) ratio and the charge by Al substituted with Si is observed it is inconsistent with the results obtained in this study. From this fact, it is estimated that the value of the surface potential obtained in this study is due to dissociation of H^+ from the SiOH site in Q^1 of the terminal chain. As described above, dissociation of H^+ of the SiOH site hardly occurs, and the possibility that the chloride ion is physically adsorbed directly to the SiOH(AlOH) site on the C-A-S-H surface which changes depending on the Ca/(Si+Al) ratio is not very high It is predicted. From this, it is suggested that the influence of the surface potential on the physical adsorption of the chloride ion can not be sufficiently evaluated by the ζ potential in the NaOH solution.

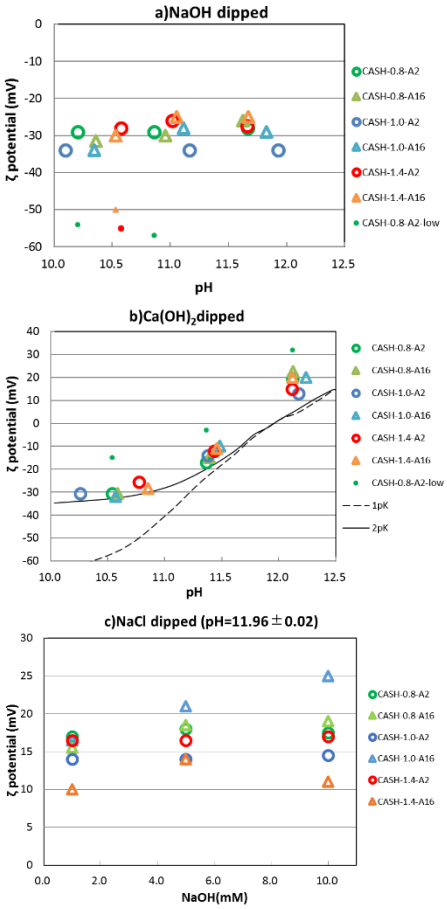

Figure 6 - Results of zeta potential measurement a)NaOH, b)$Ca(OH)_2$, c)NaCl dipped.

The ζ potential at $Ca(OH)_2$ immersion showed one peak in almost all samples. It also showed the same trend regardless of Ca/(Si+Al) ratio. These results suggest that there is no electrical difference between the $SiOCa^+$ site and the $AlOCa^+$ site generated by the Ca adsorption, and it is a similar surface site. In addition, when compared with the simulation result of Churakov et al.[4] (1pK: 1 dissociation constant, 2pK: 2 dissociation constant) shown in Figure

6, the same tendency as those having two dissociation constants was obtained . In other words, SiOH site was suggested to have two dissociation constants, although one type of charge was observed. Since the dissociation constants of these two kinds are the same as those of the ζ potential measurement regardless of the Ca/(Si+Al) ratio, it is presumed that this phenomenon is caused not by the difference between Si^{4+} and Al^{3+} but by the difference in ease of dissociation of SiOH(AlOH) site. A similar surface potential was confirmed regardless of the Ca/(Si+Al) ratio and NaCl addition amount by ζ potential measurement when immersed in NaCl. In addition, it is assumed that there is hardly any physical adsorption of chloride ions since no change is observed in the pH as well as the change in the amount of NaCl added. As a result, it is considered that physical adsorption on the C-A-S-H surface is difficult to occur in a system with high crystallinity such as a pure chemical synthesis system and in a system suppressing dissolution (Ca leaching) of a sample.

4. Conclusions

In this study, as a result of ^{27}Al MAS-NMR measurement taking into account the relaxation of the latest peak, two unknown peaks were confirmed in addition to two known peaks of the IV coordination. As a result, incorporation of Al into the Q^2_b position and the Q^2_p position was confirmed in the synthesized C-A-S-H, but also the incorporation of Al into the Q^3 position and the incorporation of Al into the Q^2_p position where Al was taken in the adjacent Q^2_b position was suggested to occur. Further, by structural analysis using ^{29}Si MAS-NMR and ^{27}Al MAS-NMR, as the Ca/(Si+Al) ratio increased, the crosslinking part decreased and the SiO_4 tetrahedral chain became shorter, and it was confirmed that the crosslinking part increased with the increase of the $CaAl_2O_4$ addition ratio and the SiO_4 tetrahedral chain became longer it was. On the other hand, the surface potential of C-A-S-H takes a similar value regardless of the Ca/(Si+Al) ratio in the case of NaOH, $Ca(OH)_2$, and NaCl dipped. It is suggested that deprotonation and physical adsorption of chloride ions at SiOH site hardly occur in the case of this study's synthesized C-A-S-H.

References

[1] Pointeau I, Reiller P, Macé N, Landesman C and Coreau N (2006) Measurement and modeling of the surface potential evolution of hydrated cement pastes as a function of degradation, Journal of Colloid and Interface Science 300, pp.33–44.

[2] R.J. Myers R. J., Hôpital E. L., John L. Provis J.L. and Lothenbach B., (2015): Effect of temperature and aluminium on calcium (alumino) silicate hydrate chemistry under equilibrium conditions Cement and Concrete Research 68, pp.83-93.

[3] Richardson I. G., (2004) Tobermorite/jennite- and tobermorite/calcium hydroxide-based models for the structure of C-S-H: applicability to hardened pastes of tricalcium silicate, β-dicalcium silicate, Portland cement, and blends of Portland cement with blast-furnace slag, metakaolin, or silica fume, Cement and Concrete Research 34, pp.1733–1777.

[4] Churakov S.V., Labbez§ C., Pegado L. and Sulpizi M. (2014), Intrinsic Acidity of Surface Sites in Calcium Silicate Hydrates and Its Implication to Their Electrokinetic Properties, The journal

of physical chemistry C, 118, pp.11752−11762.

[5] J.D. Bernal J. D., Jeffery J. W., and Taylor H. F. W: (1952) Crystallographic research on the hydration of Portland cement. A first report on investigations in progress, Mag. Concr. Res. 4 (12), pp.49-54.

[6] Faucon P., Delagrave A., Petit J. C., Richet C., MarchandJ. M. and H. Zanni (1999) Aluminum Incorporation in Calcium Silicate Hydrates (C-S-H) Depending on Their Ca/Si Ratio, J. Phys. Chem. B, 103, pp.7796-7802.

[7] Churakov S.V. and Christophe Labbez C., (2017) Thermodynamics and Molecular Mechanism of Al Incorporation in Calcium Silicate Hydrates , The journal of physical chemistry C, 121, pp.4412−4419.

[8] Pardal X., Brunet F.,Charpentier T.,‡, Pochard I. and Nonat A. (2012). ^{27}Al and ^{29}Si Solid-State NMR Characterization of Calcium-Aluminosilicate-Hydrate , Inorg. Chem., 51, pp.1827-1836.